Engineering Notes

Hierarchic Estimation for Control of Segmented-Mirror Telescopes

Douglas G. MacMynowski*
*California Institute of Technology,
Pasadena, California 91125*

I. Introduction

THE primary mirror of each of the Keck telescopes is composed of 36 hexagonal segments, with their positions accurately controlled to form a single 10-m-diam mirror.[1,2] Future optical telescopes are being designed with many more segments: The 30-m primary mirror for the Thirty Meter Telescope may have as many as 1080 segments,[3] whereas the current 100-m primary mirror design for the Overwhelmingly Large Telescope (OWL) involves 3048 segments.[4] Future ground- and spaced-based telescope concepts exist that involve between 10^4 and 10^5 segments.[5,6] In all of these concepts, at least three degrees of freedom of each segment are controlled using sensor measurements of the relative motion between neighboring segments. New algorithms are required for controlling such systems with thousands of actuators and sensors. Furthermore, whereas the control bandwidth used at Keck is sufficient to compensate for deformations due to gravity as the telescope tracks an object, future telescopes may require a higher bandwidth to compensate for wind-induced deformations,[7] further increasing the computational burden.

Adaptive optics systems for such telescopes will also likely involve many thousands of actuators and sensors. For both the primary mirror and the adaptive optics control problems, the least-squares-optimal displacement estimate at each location uses every available sensor. The computations are, therefore, dominated by the estimation of the absolute displacement errors based only on relative sensor measurements. In the case of adaptive optics, various algorithms have been developed to reduce the computational burden. These include methods based on the underlying sparse structure of the problem,[8] iterative techniques,[9] and fast Fourier transform (FFT)-based approaches (see Ref. 10). In particular, a hierarchic approach[11] can be easily extended to the primary mirror segment control problem, because the basic approach does not rely on the specific problem geometry. A local layer uses only nearby sensor information to construct an estimate of the displacement at each location. This estimator performs poorly for long length-scale deformations and can be corrected using either a global estimator on a coarser grid (a multigrid approach[12]), or an iterative scheme based on previous estimates.

II. Application

A representative geometry for a segmented primary mirror is shown in Fig. 1, with $N = 1080$ segments. Also shown are representative locations of the actuator and sensor control hardware on each segment. The out-of-plane position of each segment can be controlled by three actuators on the back of each segment, and the displacement at these locations will be used to describe the deformation of the mirror. The only information available to the control system is assumed to be measurements of the difference in displacement between neighboring segments of the mirror array, similar to those in use at the Keck telescopes.[2] Note that the differential displacement measurements cannot sense the overall uniform motion of the segment array (overall piston, tip, and tilt). In addition, if the measurements are not also sensitive to the relative dihedral angle between neighboring segments, then there is an additional focus mode that is unobservable.[13] The relationship between segment displacements $x \in \mathbb{R}^n$ ($n = 3N$) and sensor measurements $y \in \mathbb{R}^m$ can be determined from geometry[13] as

$$y = Ax + \eta \tag{1}$$

where η is sensor noise. For sufficiently large segment arrays, $m \simeq 2n$, and the problem is, thus, significantly overdetermined.

A static, rather than dynamic (Kalman filter) estimate is appropriate either if the sensor noise is small compared to the disturbances (where propagated prior information is noisier than current information), or if the control bandwidth is sufficiently lower than the structural dynamics. The latter assumption holds at Keck,[1,2] as well as for most adaptive optics systems, but may not be appropriate for future telescopes. However, the sensor noise is expected to be small,[14] and thus, it is assumed herein that the static least-squares estimate is sufficient. With noise covariance $R = \langle \eta \eta^T \rangle$ and prior displacement covariance $Q = \langle xx^T \rangle$, the least-squares estimate is

$$\hat{x}^* = K^* y = (A^T R^{-1} A + Q^{-1})^{-1} A^T R^{-1} y \tag{2}$$

In the limit of small sensor noise, for example, if $R = \rho I$, $\rho \to 0$, then

$$K^* = A^\# = \lim_{\rho \to 0} (A^T A + \rho I)^{-1} A^T \tag{3}$$

where $A^\#$ is the left pseudoinverse of A. The matrix K^* in Eq. (2) or (3) is fully populated, so that the total computations at each time step of the control are roughly $C \simeq 2n^2 \simeq 18N^2$.

Once the estimate of the local displacement is known, a controller $C(s)$ can be designed to minimize these estimated displacements using the collocated actuators. With $P(s)$ as the transfer function of the structure (displacement x for given control input), the loop transfer function with any estimator $\hat{x} = Ky$ is $P(s)C(s)L$, where $L = KA$. For integral control, a reduction in estimator gain corresponds directly to a bandwidth reduction. With the optimal-least-squares pseudoinverse in Eq. (3), $L = I - \mu\mu^T$, where $\mu \in \mathbb{R}^{n \times M}$ is a basis for the M unobservable modes.

The physical interpretation of K^* in Eq. (2) being fully populated is that, if a particular sensor measurement is nonzero, every other sensor is also required to determine whether one of the neighboring segments is too high or the other too low. Algorithms documented for the similar estimation problem in adaptive optics have decreased the computational scaling to $\mathcal{O}(n \log n)$ for iterative and FFT methods, or between $\mathcal{O}(n^{4/3})$ and $\mathcal{O}(n)$ for hierarchic approaches. For the
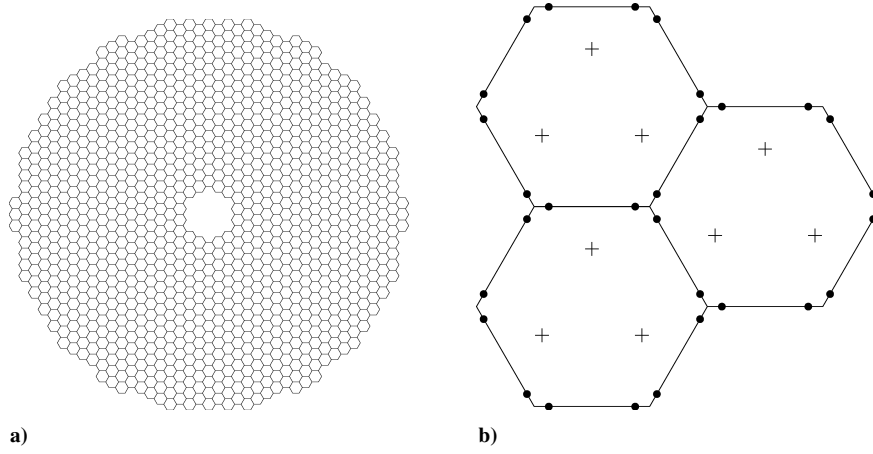
Fig. 1   Primary mirror with 15 m radius; using 1080 segments of circumscribed radius $a = 0.5$ m: a) segmentation geometry and b) three segments of mirror; locations of +, actuator and ●, intersegment sensor.
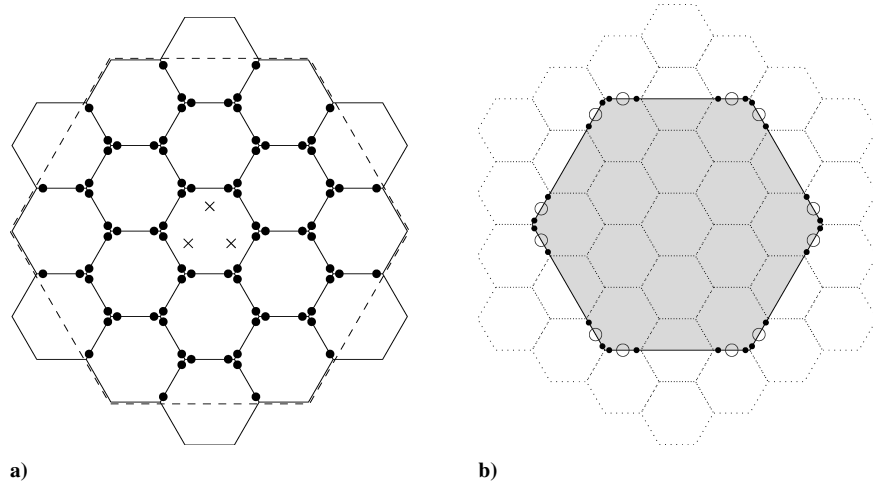

Fig. 2   Local and global layer geometry for $d = 4$: a) local region used in estimator: ×, displacement of center segment estimated based on ●, sensors within dashed region; and b) global supersegment with ····, underlying physical segments, ○, virtual sensors $\tilde{y}$ of global layer computed from ●, neighboring sensors.

adaptive optics problem solved in Ref. 11, the actuators and sensors were aligned on a uniform Cartesian grid. Modifications are required to deal with the hexagonal segmentation geometry and its associated displacements and measurements; these are described in the sequel with a summary of the approach.

III.   Local Estimate

Rather than using every sensor in the segmented-mirror array to compute the estimated displacement of a given mirror segment, consider first a local approach wherein each state estimate depends only on information within a given nearby region. The best estimate of the displacement of each segment given the sensor information available results in a local least-squares problem.

Define Ω_i as the subset of segments on which the sensors are to be used in computing the estimated displacement of segment i. Hexagonal regions of segments (Fig. 2) are chosen that are larger than the physical segments by an integer scale factor d. Interior sensors are within an area $D = d^2$ larger than a segment; including partial segments in Ω_i gives regions containing more than D segments. The geometric similarity will be essential in deriving the global hierarchic correction to the errors from the local estimate. The set Ω_i^s of sensors available to estimate the three out-of-plane displacements of the ith segment are those intersegment sensors for which both segments that influence the sensor are within Ω_i. Define Ω_i^a as the set of displacements associated with Ω_i; this satisfies $x_j \in \Omega_i^a$ if $\exists k$ such that $y_k \in \Omega_i^s$ and $A_{kj} \neq 0$. Thus, this is the set of states that influence any sensor in Ω_i^s. Define $\tilde{A}_i = A_{\Omega_i^s, \Omega_i^a}$, where the notation indicates that rows in Ω_i^s and columns in Ω_i^a are kept.

Given the subset Ω_i^s of available information, the optimal estimate of the overall state $\hat{x}|_{y \in \Omega_i^s}$ is obtained from the weighted pseudoinverse as in Eq. (2), where only the rows of A corresponding to Ω_i^s are kept. In the limit of small sensor noise (or with appropriate sparsity structure of the covariance matrices Q and R), then state estimates not in Ω_i^a will be zero, and thus, the nonzero elements of $\hat{x}|_{y \in \Omega_i^s}$ can be computed from the pseudoinverse of the truncated matrix $\tilde{A}_i$. The optimal estimate given Ω_i^s, $i = 1, \ldots, N$, is denoted $\hat{x}_\ell = K_\ell y$. Rows of K_ℓ corresponding to the displacement of segment i are nonzero only for elements corresponding to sensors in Ω_i^s. The total computation for K_ℓ is, thus, approximately $C(N) = 18DN$. Note that because A and Ω are spatially invariant away from the boundary, K_ℓ is similarly spatially invariant.

Define $\tilde{\mu}_m^i$, $m = 1, \ldots, M_i$, as an orthonormal basis for the null space of $\tilde{A}_i$. Away from the boundary, $M_i = M$, and the vectors $\tilde{\mu}_m^i$ correspond to the nullspace of the full A matrix: piston, tip, and tilt, plus a focus mode if the sensors do not measure relative dihedral between segments. For $d \geq 4$, $M_i = M$, everywhere, whereas for $d < 4$, the local estimation for some boundary segments may be underdetermined. The estimation error can be written as

$$\hat{x}_i|_{y \in \Omega_i} = \hat{x}_i|_y - \sum_{m=1}^{M_i} \left(\tilde{\mu}_m^i\right)_i \left[\left(\tilde{\mu}_m^i\right)^T x\right] + K_\ell \eta \qquad (4)$$

Thus, the average piston, tip, and tilt over Ω_i are unobservable, whereas higher-order deformations within the supersegment Ω_i are observable. This local, sparse estimator, thus, acts as a spatial high-pass filter on the actual displacement.

IV. Global Correction

Performance at low spatial frequencies can be improved by estimating the information $\tilde{\mu}_m^i$ in Eq. (4) that the local estimator does not, using a coarser global estimator (a multigrid approach). This consists of three steps: spatial filtering of the sensor information and condensing into a reduced set of data, estimating global parameters from this condensed data, and expanding these global parameters over the domain. The global parameterization is chosen to be geometrically similar to that of the underlying problem, making the addition of further layers of hierarchy a simple extension. The hexagonal supersegments of the global layer have size equal to that of the local regions Ω, as shown in Fig. 2. The three steps are then as follows:

1) Define $\tilde{y} = \Psi y$ as the relative intersegment displacement between supersegments of size Ω. This requires averaging the nearby sensors as shown in Fig. 2 and then subtracting the component of these sensor responses that is predictable from local measurements within the supersegment (to be described).

2) Define a set of global variables ξ as the displacement of the supersegments (three per), so that ξ and $\tilde{y} = A_\xi \xi$ are the displacements and sensor measurements of a similar hexagonal virtual segment geometry with resolution larger by a factor of d, and $\hat{\xi} = A_\xi^\# \tilde{y}$,

3) Define the global component of the state x as $x_g = \Phi \xi$ to estimate the error in the local estimate at each actuator location. The three degrees of freedom ξ for each supersegment are used to interpolate the global component of the displacement at each actuator location, and these are appropriately averaged to estimate the piston, tip, and tilt, that is, $(\tilde{\mu}_m^i)^T x$, $m = 1, \ldots, 3$, over each Ω_i (described later).

The combined local and global estimator is given by

$$\hat{x} = \hat{x}_\ell + \hat{x}_g$$
$$= K_\ell y + \Phi\left[A_\xi^\#(\Psi y)\right] \tag{5}$$

The additional steps in creating Ψ and Φ are critical to ensuring that the local and global estimates are complementary. The first step in creating Ψ is to define $w = \Psi_0 y$ as the average, for each global (virtual) sensor location, of the two nearby sensors. (This step is more complex for $d \neq 4$.) Removing the component of w that is predictable from local information within the global supersegment is essential for avoiding the aliasing that would otherwise occur with the spatial sampling process. This is obtained from 1) a pseudoinverse of $\tilde{A}_i$ for Ω_i aligned with the supersegment and 2) an estimate of the predicted sensor response from the predicted local displacement using Eq. (1). The first step in creating Φ is to interpolate the displacement at physical actuator locations from the displacements of the global supersegments, so that $\zeta = \Phi_0 \xi$. For segments that span two supersegments, the displacements are averaged. For each physical segment i, the piston, tip, and tilt over Ω_i are obtained by averaging the interpolated global displacement ζ. A global estimate that is orthogonal to the local estimate is obtained by computing the response at the actuator locations due to this piston, tip, and tilt.

Both Ψ and Φ are sparse. Each physical sensor is used in the computation of the global sensor response of up to seven neighboring supersegments, and each global displacement estimate $\hat{x}_g$ is interpolated from up to nine global variables $\hat{\xi}$. The computations involving Ψ and Φ are, thus, $7m \simeq 42N$ and $9n \simeq 27N$, respectively, both linear in N. With approximately N/D supersegments, the combined hierarchic estimator computations are $C(N, D) = 18(N/D)^2 + 18ND + \mathcal{O}(N)$. Optimizing gives $D = (2N)^{1/3}$ and computations $C(N) = (27/2)(2N)^{4/3} + \mathcal{O}(N)$. For the range of telescope concepts in the near future between $\sim$800 and $\sim$4000 segments, then $d = 4$ is the optimum integer value. A different control bandwidth can be obtained for different spatial scales by computing the control as the sum of contributions from the different hierarchic layers. Thus, rather than $u = C(s)\hat{x}$, choose $u = C_\ell(s)\hat{x}_\ell + C_g(s)\hat{x}_g$. If the bandwidth requirements are driven by frozen turbulence wind across the primary mirror, then the required bandwidth is approximately proportional to the wave number.[7] If the global computations

can thus be performed d times slower than the local computations, the optimization yields computational scaling of $N^{9/7}$.

The approximation to the full least-squares estimator introduces errors. These can be mitigated as in any multigrid scheme by iterating the estimation on the residual error $e = y - A\hat{x}$, so that the estimate at the kth iteration is

$$\hat{x}_k = \hat{x}_{k-1} + K e_{k-1} \tag{6}$$

The error between the hierarchic and full estimator converges to zero, although the number of iterations required for a given error will depend on the size of the problem.

The iteration in Eq. (6) has an additional interpretation if applied directly to the local, rather than the combined hierarchic, estimator. With no global estimator, rewrite Eq. (6) as

$$\hat{x}_k = K_\ell y_k + G\hat{x}_{k-1} \tag{7}$$

where $G = I - K_\ell A$ has nonzero elements for segment i only for previous estimates in the set Ω_i^a. This alternate iterative approach corrects the local estimator by estimating the "missing" information $(\tilde{\mu}_m^i)_i[(\tilde{\mu}_m^i)^T x]$, $m = 1, \ldots, 3$, using previous state estimates $\hat{x}$. Equation (7) naturally includes information from prior sample/control iterations, with potentially multiple subiterations between these. The derivation and analysis in this case are identical to the adaptive optics problem.[11] This iterative scheme converges to the full estimate in steady state and acts as a temporal low-pass filter on the global information. Because only local values of $\hat{x}$ are required in addition to the local sensor information, a distributed implementation would be feasible with this approach.

V. Simulation Results

The performance of the hierarchic and iterative estimators is evaluated for the 1080-segment mirror geometry shown in Fig. 1, by using $d = 4$. The virtual supersegments of the hierarchic geometry are overlaid on the physical geometry in Fig. 3.

The A matrix for the physical geometry and the supersegment geometry are obtained as in Ref. 13, with pure displacement sensors not sensitive to relative segment dihedral angle. The local and global estimates are obtained and combined, giving computations per iteration of Eq. (6) of 2.3% of those of the full estimator. The convergence of the estimation error $\|\hat{x}_k - \hat{x}^*\|_2$ is shown in Fig. 4, assuming equal and uncorrelated displacement covariance. Using four iterations for the hierarchic estimate, the behavior of this and the local and global estimators for low wave number deformations is plotted in Fig. 5. The loop gain projected onto Zernike basis
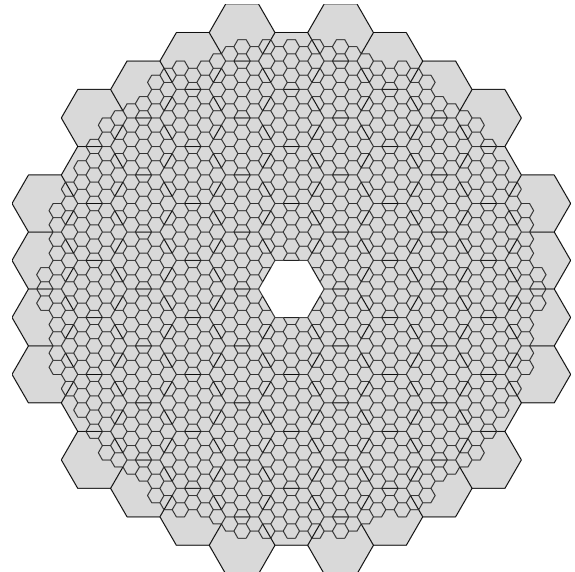

Fig. 3 Eighty-four virtual supersegments of hierarchic estimator overlaid on the 1080-segment mirror geometry from Fig. 1.
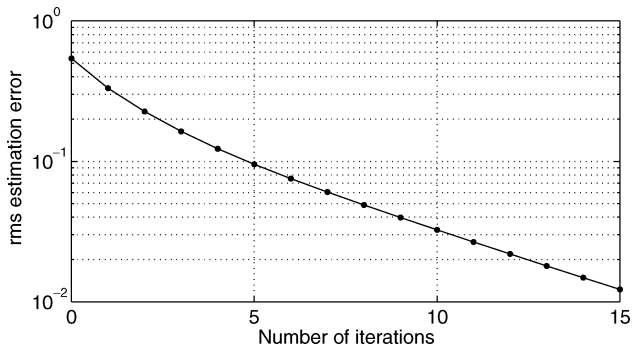
Fig. 4 Convergence of estimation error $\|\hat{x}_k - \hat{x}^*\|_2$ with k iterations.
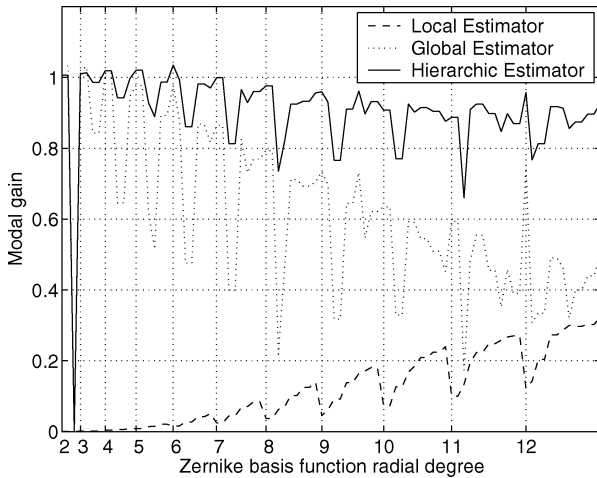

Fig. 5 Modal gains for local and hierarchic control for geometry in Fig. 3, as function of Zernike basis function. The hierarchic estimator is shown for four iterations.

functions ϕ_k is plotted, that is, $L_k = \phi_k^T(KA)\phi_k$. The unobservable overall piston, tip, and tilt are not shown; the first three modes are astigmatism (two modes) and focus, which is not observable with these sensors. The nonmonotonic nature of the modal gains is largely a result of the ordering of Zernike basis functions by increasing radial degree rather than by increasing wave number. Note that for the 91 lowest spatial wave number modes shown in Fig. 5 the local estimator gain is low, but high wave number motion is accurately estimated. With the hierarchic estimator gain K (with no iterations), the diagonal elements of $L = KA$ are on average 5% below unity, with a standard deviation of 3%, additional iterations improve this performance further.

VI. Conclusions

Ground-based optical telescopes are currently being designed with segmented primary mirrors composed of thousands of hexagonal segments whose displacement must be accurately controlled. Estimating each segment displacement from relative intersegment motion leads to a fully coupled problem with a potentially significant computational burden. A hierarchic (multigrid) estimation approach

developed for adaptive optics has been extended to this application. High spatial wave number deformations are estimated using local measurements of the relative displacements of nearby segments. This displacement estimate is augmented with a global estimate using a geometrically similar but coarser, virtual segmentation geometry. For a 1080-segment geometry, the resulting architecture reduces the computational burden by a factor of 10 with no significant loss in performance, or by a larger factor with some performance penalty. A full evaluation of the closed-loop performance requires models of the telescope structure and disturbance environment.

References

[1] Aubrun, J.-N., Lorell, K. R., Mast, T. S., and Nelson, J. E., "Dynamic Analysis of the Actively Controlled Segmented Mirror of the W. M. Keck Ten-Meter Telescope," *IEEE Control Systems Magazine*, Vol. 7, No. 6, 1987, pp. 3–10.

[2] Jared, R. C., Arthur, A. A., Andreae, S., Biocca, A., Cohen, R. W., Fuertes, J. M., Franck, J., Gabor, G., Llacer, J., Mast, T., Meng, J., Merrick, T., Minor, R., Nelson, J., Orayani, M., Salz, P., Schaefer, B., and Witebsky, C., "The W. M. Keck Telescope Segmented Primary Mirror Active Control System," *Advanced Technology Optical Telescopes IV*, edited by L. D. Barr, Vol. 1236, *Proceedings of the SPIE*, Society of Photo-Optical Instrumentation Engineers, Bellingham, WA, 1990, pp. 996–1008.

[3] Nelson, J. E., "Progress on the California Extremely Large Telescope (CELT)," *Future Giant Telescopes*, edited by R. P. Angel and R. Gilmozzi, Vol. 4080, *Proceedings of the SPIE*, Society of Photo-Optical Instrumentation Engineers, Bellingham, WA, 2002, pp. 47–59.

[4] Dierickx, P., Brunetto, E., Comeron, F., Gilmozzi, R., Gonte, F., Koch, F., le Louarn, M., Monnet, G., Spyromilio, J., Surdej, I., Verinaud, C., and Yaitskova, N., "OWL Phase A Status Report," *Ground-Based Telescopes*, edited by J. M. Oschmann, Vol. 5489, *Proceedings of the SPIE*, Society of Photo-Optical Instrumentation Engineers, Bellingham, WA, 2004, pp. 391–406.

[5] Padin, S., "Design Considerations for a Highly Segmented Mirror," *Applied Optics*, Vol. 42, No. 16, 2003, pp. 3305–3312.

[6] Dekany, R. G., MacMartin, D. G., Chanan, G. A., and Troy, M., "Advanced Segmented Silicon Space Telescope (ASSiST)," *Highly Innovative Space Telescope Concepts*, edited by H. A. MacEwen, Vol. 4849, *Proceedings of the SPIE*, Society of Photo-Optical Instrumentation Engineers, Bellingham, WA, 2002, pp. 103–111.

[7] Padin, S., "Wind-induced Deformations in a Segmented Mirror," *Applied Optics*, Vol. 41, No. 13, 2002, pp. 2381–2389.

[8] Ellerbroek, B. L., "Efficient Computation of Minimum-Variance Wave-Front Reconstructors with Sparse Matrix Techniques," *Journal of the Optical Society of America A*, Vol. 19, No. 9, 2002, pp. 1803–1816.

[9] Gilles, L., Vogel, C. R., and Ellerbroek, B. L., "Multigrid Preconditioned Conjugate-Gradient Method for Large-Scale Wave-front Reconstruction," *Journal of the Optical Society of America A*, Vol. 19, No. 9, 2002, pp. 1817–1822.

[10] Poyneer, L. A., Gavel, D. T., and Brase, J. M., "Fast Wavefront Reconstruction in Large Adaptive Optics Systems with Use of the Fourier Transform," *Journal Optical Society of America A*, Vol. 19, No. 10, 2002, pp. 2100–2111.

[11] MacMartin, D. G., "Local, Hierarchic, and Iterative Reconstructors for Adaptive Optics," *Journal of the Optical Society of America A*, Vol. 20, No. 6, 2003, pp. 1084–1093.

[12] Wesseling, P., *An Introduction to Multigrid Methods*, Wiley, 1992; corrected reprint, R. T. Edwards, Chichester, England, U.K., 2004.

[13] Chanan, G., MacMartin, D. G., Nelson, J., and Mast, T., "Control and Alignment of Segmented-Mirror Telescopes: Matrices, Modes, and Error Propagation," *Applied Optics*, Vol. 43, No. 6, 2004, pp. 1223–1232.

[14] MacMartin, D. G., and Chanan, G., "Measurement Accuracy in Control of Segmented-Mirror Telescopes," *Applied Optics*, Vol. 43, No. 3, 2004, pp. 608–615.